Optimal Design of Coreless Axial Flux PM Machines Using a Hybrid Machine Learning and Differential Evolution Method

Matin Vatani
SPARK Lab, Pigman Eng. College
University of Kentucky
Lexington, KY, USA
matin.vatani@uky.edu

David R. Stewart
SPARK Lab, Pigman Eng. College
University of Kentucky
Lexington, KY, USA
david.stewart@uky.edu

Pedram Asef
Advanced Propulsion Lab, Mech. Eng. Dept.
University College London
London, UK
pedram.asef@ucl.ac.uk

Dan M. Ionel
SPARK Lab, Pigman Eng. College
University of Kentucky
Lexington, KY, USA
dan.ionel@ieee.org

***Abstract*—Coreless stator axial flux permanent magnet (AFPM) machines require computationally intensive three-dimensional finite element analysis (FEA) for accurate performance evaluation, making optimization time-consuming and impractical for large-scale design studies. This paper presents a hybrid optimization approach that integrates differential evolution (DE) with artificial neural networks (ANNs) to accelerate the optimization of coreless AFPM machines. In this method, DE-driven FEA simulations generate a dataset used to train an ANN surrogate model, significantly reducing reliance on direct FEA computations. The effectiveness of this approach is demonstrated through a multi-objective DE optimization, where the ANN's predictions are validated against FEA results. The proposed hybrid method substantially reduces computational cost while maintaining accuracy, providing an efficient solution for electric motor design optimization.**

***Index Terms*—Meta-modeling, artificial neural network, deep learning, axial flux, coreless stator, Halbach PM array.**

I. Introduction

Axial flux permanent magnet (AFPM) machines offer higher potential power density and specific power than their more common radial flux counterparts [1–3], making them ideal for applications requiring compact design, excellent torque density, enhanced energy efficiency, and better cooling flexibility. Their disk-shaped structure allows for high pole numbers [4], making them well-suited for low-speed applications. Advancements in solid-state switches and power electronic cooling have mitigated high switching frequency losses, positioning AFPM machines as strong candidates for high-speed applications, as for example demonstrated in [5–7].

More novel AFPM machine topologies, such as yokeless and segmented armature (YASA) and coreless stator designs, have further enhanced the advantages of this class of electric machines. The YASA topology, first introduced in [8], eliminates the stator yoke, reducing motor mass and core losses. The YASA motor enables more efficient cooling strategies, such as immersing stator segments in an enclosed coolant, as discussed in [9, 10]. Axial flux machine with YASA topology is actively explored for various applications, ranging from automotive to aerospace, as exemplified in [11–14].

Coreless stator AFPM machines are derived from the YASA topology by eliminating the stator teeth segments and placing the windings directly in the air-gap. The torque production in coreless stator machines is governed by the Lorentz force theorem through the interaction between current-carrying conductors and the rotor's magnetic field [15–17]. This topology has been shown to potentially achieve high specific power density and facilitate direct winding cooling due to improved accessibility. These advantages make coreless stator AFPM machines particularly well-suited for aerospace [18–20].

The coreless stator configuration enables a modular structure that enhances fault tolerance, as demonstrated in [21]. This design allows decoupled stators to be connected to different power sources or loads, as exemplified in [22]. The absence of a stator core and the low armature field reduce normal forces between the stator and rotor, resulting in a more straightforward mechanical structure to manage these forces. Accordingly, coreless stator AFPM machines have been proposed for large direct-drive wind turbine generators, benefiting from a lighter mechanical structure [23, 24].

Due to the flux pattern in AFPM machines, three-dimensional (3D) FEA modeling is required for accurate performance calculations [25, 26]. The 3D FEA modeling can be time-consuming and costly, especially when optimization is required, as solving hundreds or even thousands of candidates is necessary to determine the optimal Pareto front. To accelerate the design and computation process, alternative approaches have been explored, such as equivalent linear 2D modeling of AFPM machines [15], and more recently, machine learning

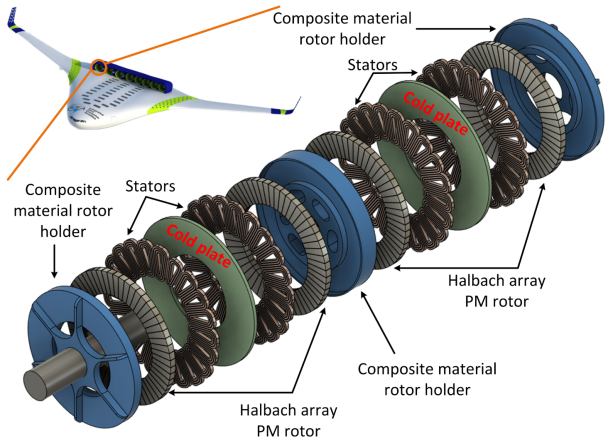

Fig. 1. Exploded view of the dual-stage coreless axial flux PM machine featuring double-sided Halbach array rotors, dual stators, and integrated cooling systems proposed for electric aircraft propulsion.

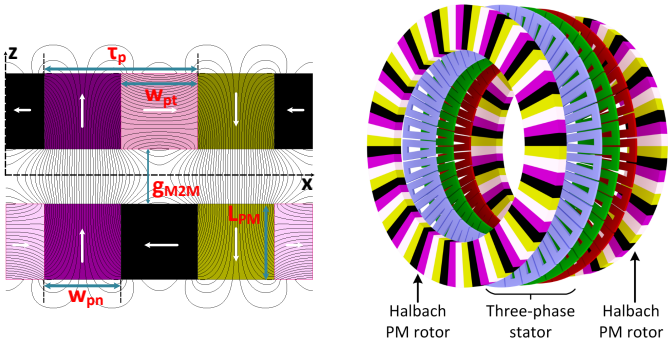

(a) (b)

Fig. 2. Coreless AFPM machine used in the optimization case study, illustrating (a) the rotor's geometrical parameters for the Halbach array at an arbitrary radial cross-section, employed for analytical flux density calculations, and (b) an exploded view of the motor with the double-sided Halbach rotors and the three-layer stator.

(ML) techniques have shown significant potential in this area [27].

Applications of ML and artificial intelligence (AI) techniques for calculating key performance indicators (KPIs) in radial flux PM machines have been explored in the literature. For instance, in [28], a dataset of 10,000 FEA-simulated design candidates with varying geometric parameters was used to train and evaluate a ML model for performance prediction in a radial flux surface-mounted PM machine. Similarly, studies such as [29, 30] employed a variational autoencoder to optimize two machine types: an induction motor, with training data generated through analytical calculations of multiple design candidates, and an interior PM radial flux machine, where training data was derived from magnetostatic 2D FEA simulations.

This paper focuses on the high-speed design optimization and scaling of coreless stator AFPM machines for electric aircraft propulsion as part of the National Aeronautics and Space Administration (NASA) Integrated Zero Emission Aviation (IZEA) program. The primary aircraft design specifications, including power requirements during different operational modes, are presented in [31], while the multi-physics design of the electric machine is detailed in [18]. The project necessitates evaluating multiple variations of the proposed electric motor across different power and speed ratings, a task that is computationally extensive and time-consuming when relying solely on FEA-based optimization.

Modeling AFPM machines is inherently more complex than radial flux machines due to curvature and edge effects, which become even more significant in coreless stator AFPM machines due to the absence of the stator core and larger airgap. Therefore, fine-tuning the ML model to capture these variations and nonlinearities accurately is essential. The effectiveness of ML in predicting KPIs for coreless AFPM machines has been demonstrated in [32] using a trained metamodel, and this paper proposes a fast optimization method based on ML modeling.

II. Machine Topology and Operating Principle

The proposed motor concept for electric aircraft propulsion, illustrated in Fig. 1, is a dual-stage AFPM machine with an integrated cooling structure. Each stage comprises a coreless stator with double-sided Halbach array PM rotors and dual three-phase stators, independently connected to separate power electronic systems to enhance operational reliability. The motor is designed to operate under high electric loading conditions, supported by a cryogenic thermal management system that maintains an operating temperature of -140°C. The cooling structure features an aluminum nitride axial disk positioned between the two stators in each stage, incorporating radial channels within the cold plate to facilitate the high-pressure circulation of liquid hydrogen.

The proposed electric propulsion concept is designed for a large manned electric aircraft with a seating capacity of over 100 passengers. The baseline design specifies eight motors, each delivering 2 MW of power during takeoff. The project also explores alternative configurations, varying the number of motors and power ratings to identify the optimal combination for overall aircraft performance. This approach requires multiple motor designs, necessitating a multi-physics, 3D optimization framework. The inherent complexity of this problem makes the optimization process both time-intensive and technically demanding. To address these challenges, this paper presents a combined optimization methodology to accelerate the design and scaling of coreless AFPM machines, enabling efficient exploration of the design space.

To implement and assess the feasibility of the combined optimization method, a coreless stator AFPM machine topology is selected. This topology avoids the complexities of multi-physics problems, allowing the focus to remain solely on electromagnetic performance. Once the effectiveness of the developed optimization method is validated, it can be extended to the original, more complex concept. The selected coreless stator AFPM machine, depicted in Fig. 2, features a double-sided Halbach array PM rotor with a three-layer printed

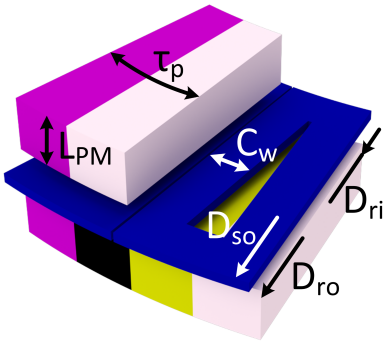

Fig. 3. Cross-sectional views of the coreless AFPM machine, with labeled geometric parameters.

circuit board (PCB) stator, where each layer corresponds to an individual phase.

The configuration of the Halbach array PM rotors, represented as a cylindrical cross-section at an arbitrary radius of the machine, is illustrated in Fig. 2a. The no-load normal component of flux density in the air-gap can be determined using [15]:

$$B_n = 2B_r \sum_{i=0}^{\infty} \frac{\sin(\epsilon n\pi/m)}{n\pi/m}\left[1-\exp\left(\frac{-n\pi L_{pm}}{\tau_p}\right)\right] \exp\left(\frac{-n\pi g_{M2M}}{2\tau_p}\right)\cosh\left(\frac{n\pi y}{\tau_p}\right)\sin\left(\frac{n\pi x}{\tau_p}\right), \quad (1)$$

where B_r represents the remanence of the PMs, and ϵ is a constant, typically set to one. The term $n = 1 + mi$, where m denotes the number of PMs per wavelength, and i represents the harmonic order. L_{PM} is the length of the PM, τ_p is the pole pitch width, and g_{M2M} is the magnet-to-magnet gap. The coordinates y and x correspond to the positions in the Y and X directions, respectively.

The force in a coreless machine can be derived using the Lorentz force equation [33], as shown in equation 2. Subsequently, the torque is calculated using equation 3.

$$F = \int_v J \times B \, dv, \quad (2)$$

$$T_{avg} = K_1 N_t I_p k_w B_1 P D_{ro}^2 \frac{\lambda^2 - 1}{8\lambda^2}, \quad (3)$$

where J is the current density, B_n is the flux density amplitude, K_1 is a constant dependent on the fraction of the total model being analyzed, N_t is the number of turns per coil, I_P is the peak current value, K_w is the winding factor, D_{ro} is the outer diameter, and λ is the ratio of the outer to the inner radii. As the coreless AFPM machine under study lacks a ferromagnetic core, saturation effects are absent. Consequently, the generated torque scales linearly with the input current.

Table I
INDEPENDENT VARIABLES AND CORRESPONDING LIMITS FOR THE CAFPM MACHINE UNDER STUDY.

Variable	Min.	Max.
Rotor diameter ratio, $K_{dr} = \frac{D_{ro}-D_{ri}}{D_{ro}}$	0.15	0.35
PM axial length ratio, $K_{PM} = \frac{L_{PM}}{\tau_p}$	0.15	0.50
Magnet-to-magnet gap ratio, $K_g = \frac{g_{M2M}}{\tau_p}$	0.14	0.75
Coil side width ratio, $K_{cw} = \frac{4C_w}{\tau_p D_{ri}}$	0.77	1.00
Overhang ratio, $K_{oh} = \frac{D_{so}-D_{ro}}{2C_w}$	0.00	1.00

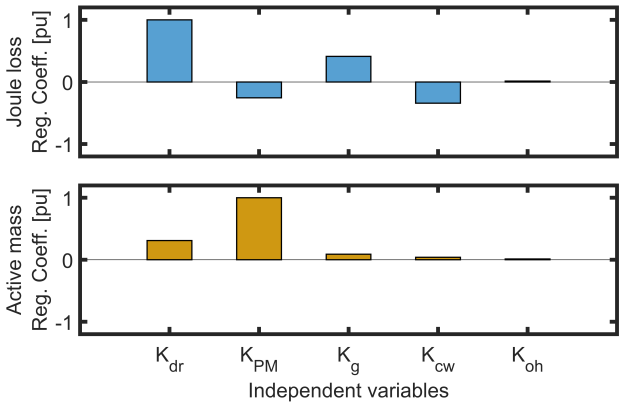

Fig. 4. The effect of optimization variables on active mass and Joule loss, depicted through per-unit regression coefficients.

III. HIGH-FIDELITY SENSITIVITY ANALYSIS AND OPTIMIZATION PROCESS

The primary objectives for electric machines designed for electric aircraft propulsion are achieving high specific power density (kW/kg) and ultra-high efficiency. Hence, the optimization process in this study focuses on minimizing the active component mass, including PMs and stator windings, and Joule loss. A two-step analysis approach is employed to ensure all optimized designs meet the required torque output. Initially, designs are analyzed using a predefined current density, which is then scaled during post-processing to guarantee the production of the 19 Nm rated torque.

Performance objectives and other indices are evaluated using 3D FEA, which leverages symmetry and matching boundary conditions inherent to the topology of the coreless AFPM machine. This allows the simulation of only one pole, one coil of a single phase, and half the machine axially. A computationally efficient FEA (CE-FEA) technique is applied, which reduces simulation time by requiring torque calculations at just two points in the transient analysis.

A sensitivity analysis was performed to evaluate the impact of design variables on the performance objectives of the coreless AFPM machine. Using a full factorial design of experiments (DoE), normalized regression coefficients were computed to create response surfaces, which reveal how

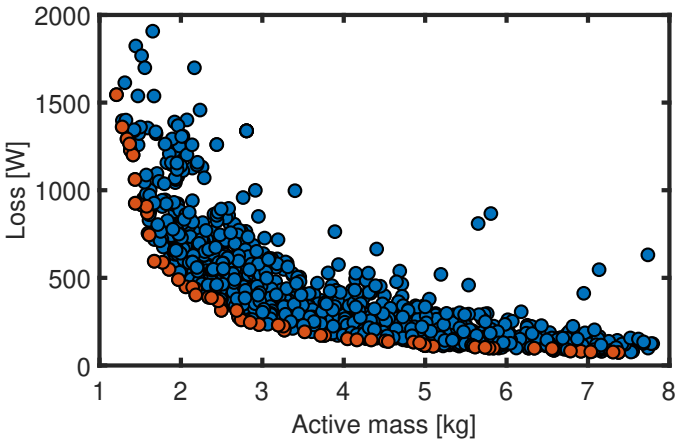

Fig. 5. All design candidates evaluated using 3D FEA, with orange markers representing the Pareto-optimal designs.

parameter variations within their allowable ranges influence performance metrics [34]. Positive coefficients indicate a proportional increase in the response value, while negative coefficients suggest a decrease, with larger magnitudes signifying greater variable influence. The effects of these variables on active mass and Joule loss are illustrated in Fig. 4.

Key findings show that increasing rotor radial length and magnet-to-magnet gap raises Joule loss, while larger magnet axial length reduces it by enhancing magnetic loading. The rise in Ampere-turn from a wider M2M gap does not sufficiently offset the decline in air-gap flux density, leading to higher Joule losses. Increasing coil side width boosts stator ampere-turn, reducing current density requirements and thus lowering Joule loss.

A large-scale multi-objective differential evolution (MODE) algorithm was employed to optimize the coreless AFPM machine. The geometric design variable search space, detailed in Table I, is slightly broader than the ranges suggested by the parametric studies in [19]. This broader range enables a more comprehensive exploration of design variables while maintaining consistency with each variable's impact on the performance objectives and compliance with geometric constraints. For instance, although an increased rotor radial length—associated with K_{dr}—can enhance output power, the specific power declines significantly when K_{dr} exceeds 0.35. A similar trend is observed for PM axial lengths greater than half the pole pitch.

A population size of 40 individuals per generation was chosen, significantly exceeding the number of independent variables to ensure robust optimization. The optimization results, illustrated in Fig. 5, highlight the Pareto-optimal solutions, marked in red. These designs represent trade-offs among the objectives and maintain consistent torque output while varying in current density.

IV. Optimization Method

The proposed combined DE and artificial neural network (ANN) optimization algorithm is shown in Fig. 6. To implement this, an ANN meta-model was developed using TensorFlow [35] and trained on the results of 3D FEA from DE optimization to predict the torque output of various coreless AFPM machine designs. By leveraging feasible designs obtained from the DE optimization, the ANN may rapidly generate additional designs within the optimal range. This approach can significantly reduce computational burden by serving as a surrogate model, potentially reducing reliance on time-intensive 3D FEA simulations.

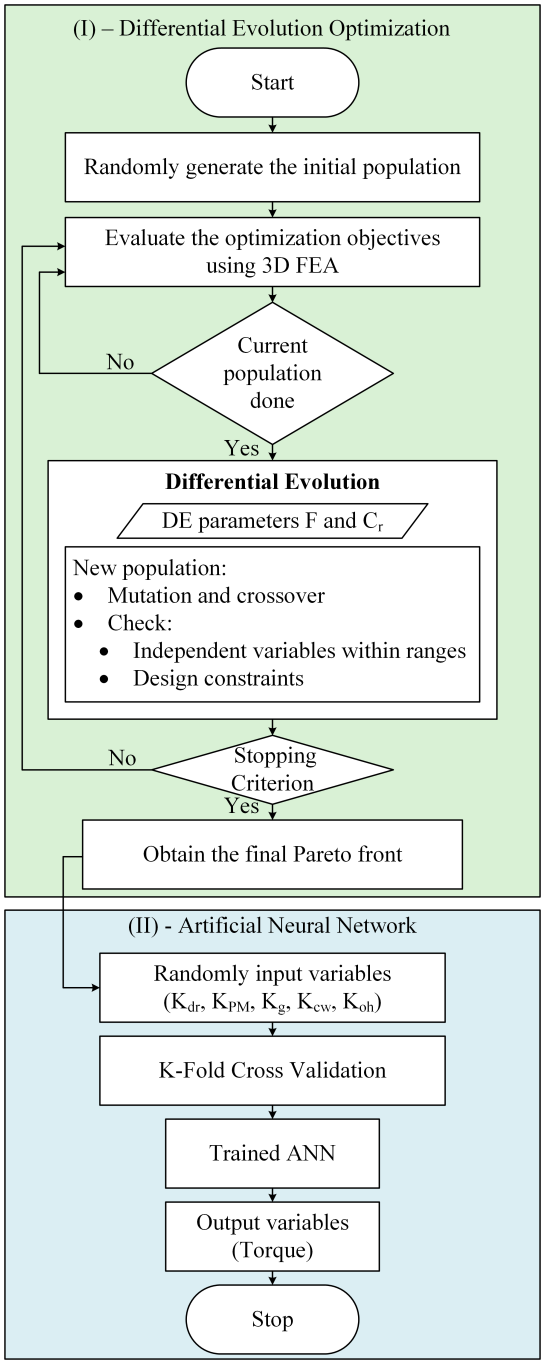

Fig. 6. The proposed hybrid optimization algorithm, combining FEA-based differential evolution and artificial neural network.

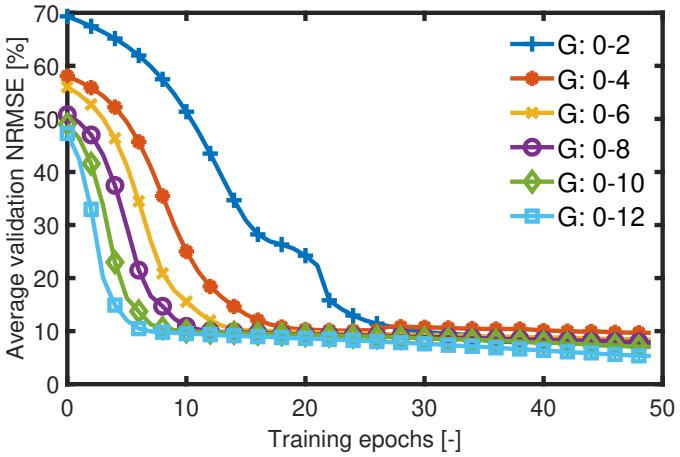

Fig. 7. Progression of the RMSE across 50 epochs for various training sets.

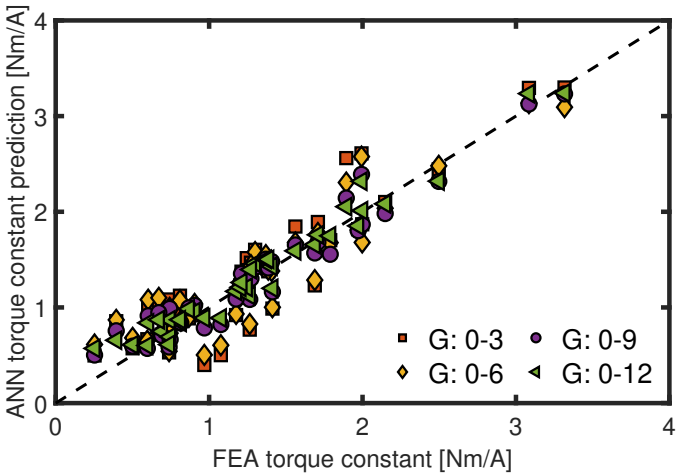

Fig. 8. Regression curve comparing the torque predicted by the ANN and 3D FEA.

To evaluate the feasibility of the proposed optimization method, ANN models were developed using datasets derived from varying numbers of generations of DE optimization results. Each ANN model was then tested against the FEA designs from the final generation of the DE optimization. This comparison provides insights into the minimum number of DE optimization generations needed to train an accurate ANN model capable of functioning as a reliable surrogate method.

The normalized root mean square error (NRMSE) values for ANN models trained with datasets from varying numbers of DE generations were compared over 50 epochs, as shown in Fig. 7. Models trained with more DE generations exhibited a faster reduction in NRMSE, particularly within the first ten epochs when using data from 12 DE generations. Following this rapid decline, the NRMSE stabilized below 8%, indicating satisfactory accuracy and effective convergence.

The accuracy of the torque constant prediction of ANNs trained on datasets generated from different numbers of DE generations compared to torque constant values obtained through FEA in Fig. 8. In line with expectation, the correlation between reference FEA and ANN improves with more generations, which is noticeable at around the rated torque constant of 2 Nm/A. With a larger number of generations, the error between the ANN and FEA results remains within a ±10% range, which may be considered acceptable for a first-level approximation. Notably, even the ANN trained with data from only nine generations stays within this ±10% margin, while models trained on datasets from more generations indicate even greater accuracy. For instance, an ANN trained on data from 40 generations was investigated in [32], achieving an error margin as low as ±3% relative to the FEA results.

V. Conclusion

This paper introduced a hybrid optimization approach that combines the DE algorithm with ANNs to streamline the design process for electric motors. The DE algorithm generates a database of designs analyzed through 3D electromagnetic FEA, while the ANN creates a surrogate meta-model to potentially replace computationally intensive FEA simulations. This method can be applied to optimize electric machines as exemplified for coreless AFPM machines.

The ANN meta-model, which was developed using a large-scale dataset of over 1,500 designs, indicated satisfactory validation results, making it a viable alternative for ultra-fast optimization. The study explored the minimum number of DE generations and design candidates required to train a satisfactorily accurate ANN model. Results revealed that a meta-model with error contained within a ±10% band can be achieved using data from nine DE generations, potentially reducing computational demands while maintaining design efficacy.

Acknowledgment

University of Kentucky students' research has been supported by the National Aeronautics and Space Administration (NASA) University Leadership Initiative (ULI) award #80NSSC22M0068. The support of ANSYS Inc., University of Kentucky the L. Stanley Pigman Chair in Power endowment is also gratefully acknowledged. Any findings and conclusions expressed herein are those of the authors and do not necessarily reflect the views of the sponsor organizations. Special thanks are due to our colleague, Ph. D. student Diego A. Lopez Guerrero, for contributions to the concept multi-stage electric motor.

References

[1] M. Aydin, S. Huang, and T. Lipo, "Axial flux permanent magnet disc machines: A review," *Conf. Record of SPEEDAM*, 01 2004.

[2] F. Nishanth, J. Van Verdeghem, and E. L. Severson, "A review of axial flux permanent magnet machine technology," *IEEE Transactions on Industry Applications*, 2023.

[3] F. G. Capponi, G. De Donato, and F. Caricchi, "Recent advances in axial-flux permanent-magnet machine technology," *IEEE Transactions on Industry Applications*, vol. 48, no. 6, pp. 2190–2205, 2012.

[4] J. F. Gieras, R.-J. Wang, and M. J. Kamper, *Axial flux permanent magnet brushless machines*. Springer Science & Business Media, 2008.

[5] R. Hill-Cottingham, P. Coles, J. Eastham, F. Profumo, A. Tenconi, G. Gianolio, and M. Cerchio, "Plastic structure multi-disc axial flux PM motor," in *Conference Record of the 2002 IEEE Industry Applications Conference. 37th IAS Annual Meeting (Cat. No.02CH37344)*, vol. 2, 2002, pp. 1274–1280 vol.2.

[6] F. Profumo, A. Tenconi, M. Cerchio, J. Eastham, and P. Coles, "Axial flux plastic multi-disc brushless PM motors: performance assessment," in *Nineteenth Annual IEEE Applied Power Electronics Conference and Exposition, 2004. APEC'04.*, vol. 2. IEEE, 2004, pp. 1117–1123.

[7] F. Y. Notash, M. Vatani, J. He, and D. M. Ionel, "Model predictive control of 5l-anpc inverter fed coreless AFPM motor with mitigated cmv in electric aircraft propulsion," in *2024 IEEE Energy Conversion Congress and Exposition (ECCE)*. IEEE, 2024, pp. 2498–2505.

[8] T. J. Woolmer and M. D. McCulloch, "Axial flux permanent magnet machines: A new topology for high performance applications," in *IET Hybrid Vehicle Conference 2006*. IET, 2006, pp. 27–42.

[9] C. Jenkins, S. Jones-Jackson, I. Zaher, G. Pietrini, R. Rodriguez, J. Cotton, and A. Emadi, "Innovations in axial flux permanent magnet motor thermal management for high power density applications," *IEEE Transactions on Transportation Electrification*, vol. 9, no. 3, pp. 4380–4405, 2023.

[10] R. Camilleri and M. D. McCulloch, "Integrating a heat sink into concentrated wound coils to improve the current density of an axial flux, direct liquid cooled electrical machine with segmented stator," *Energies*, vol. 14, no. 12, p. 3619, 2021.

[11] A. Allca-Pekarovic, P. J. Kollmeyer, A. Forsyth, and A. Emadi, "Experimental characterization and modeling of a yasa p400 axial flux PM traction machine for performance analysis of a chevy bolt ev," *IEEE Transactions on Industry Applications*, vol. 60, no. 2, pp. 3108–3119, 2023.

[12] D. Winterborne, N. Stannard, L. Sjöberg, and G. Atkinson, "An air-cooled yasa motor for in-wheel electric vehicle applications," *IEEE Transactions on Industry Applications*, vol. 56, no. 6, pp. 6448–6455, 2020.

[13] T. Bingham, M. Moore, T. De Caux, and M. Pacino, "Design, build, test and flight of the world's fastest electric aircraft," *IET Electrical Systems in Transportation*, vol. 12, no. 4, pp. 380–402, 2022.

[14] D. Talebi, M. C. Gardner, S. V. Sankarraman, A. Daniar, and H. A. Toliyat, "Electromagnetic design characterization of a dual rotor axial flux motor for electric aircraft," *IEEE Transactions on Industry Applications*, vol. 58, no. 6, pp. 7088–7098, 2022.

[15] M. Vatani, Y. Chulaee, J. F. Eastham, and D. M. Ionel, "Analytical and fe modeling for the design of coreless axial flux machines with Halbac array and surface PM rotors," in *2024 IEEE Energy Conversion Congress and Exposition (ECCE)*. IEEE, 2024, pp. 5205–5211.

[16] N. Chayopitak and D. G. Taylor, "Performance assessment of air-core linear permanent-magnet synchronous motors," *IEEE transactions on magnetics*, vol. 44, no. 10, pp. 2310–2316, 2008.

[17] S. G. Min and B. Sarlioglu, "3-d performance analysis and multiobjective optimization of coreless-type PM linear synchronous motors," *IEEE Transactions on Industrial Electronics*, vol. 65, no. 2, pp. 1855–1864, 2017.

[18] M. Vatani, Y. Chulaee, A. Mohammadi, D. R. Stewart, J. F. Eastham, and D. M. Ionel, "On the optimal design of coreless AFPM machines with Halbach array rotors for electric aircraft propulsion," in *2024 IEEE Transportation Electrification Conference and Expo (ITEC)*. IEEE, 2024, pp. 1–6.

[19] M. Vatani, J. F. Eastham, and D. M. Ionel, "Multi-disk coreless axial flux permanent magnet synchronous motors with surface PM and Halbac array rotors for electric aircraft propulsion," in *2024 IEEE Energy Conversion Congress and Exposition (ECCE)*. IEEE, 2024, pp. 4986–4992.

[20] F. Marcolini, G. De Donato, F. G. Capponi, M. Incurvati, and F. Caricchi, "Novel multiphysics design methodology for coreless axial flux permanent magnet machines," *IEEE Transactions on Industry Applications*, 2023.

[21] D. D. Lewis, D. R. Stewart, M. Vatani, O. A. Badewa, A. Mohammadi, and D. M. Ionel, "Fault-tolerant topologies with Halbac array and PM-free multi-stage multi-module electric machines for electric aircraft propulsion," in *2024 IEEE Energy Conversion Congress and Exposition (ECCE)*. IEEE, 2024, pp. 2524–2528.

[22] M. Vatani, Y. Chulaee, J. F. Eastham, X. Pei, and D. M. Ionel, "Multi-wound axial flux generators with Halbac array rotors," in *2024 IEEE Energy Conversion Congress and Exposition (ECCE)*. IEEE, 2024, pp. 5199–5204.

[23] M. A. Mueller and A. S. McDonald, "A lightweight low-speed permanent magnet electrical generator for direct-drive wind turbines," *Wind Energy: An International Journal for Progress and Applications in Wind Power Conversion Technology*, vol. 12, no. 8, pp. 768–780, 2009.

[24] M. Vatani, A. Mohammadi, D. Lewis, J. F. Eastham, and D. M. Ionel, "Coreless axial flux Halbac array permanent magnet generator concept for direct-drive wind turbine," in *2023 12th International Conference on Renewable Energy Research and Applications (ICRERA)*. IEEE, 2023, pp. 612–617.

[25] M. Gulec and M. Aydin, "Implementation of different 2d finite element modelling approaches in axial flux permanent magnet disc machines," *IET Electric Power Applications*, vol. 12, no. 2, pp. 195–202, 2018.

[26] J. R. Bumby, R. Martin, M. Mueller, E. Spooner, N. Brown, and B. Chalmers, "Electromagnetic design of axial-flux permanent magnet machines," *IEE Proceedings-Electric Power Applications*, vol. 151, no. 2, pp. 151–160, 2004.

[27] P. Asef and C. Vagg, "A physics-informed bayesian optimization method for rapid development of electrical machines," *Scientific Reports*, vol. 14, no. 1, p. 4526, 2024.

[28] B. Poudel and E. Amiri, "Deep learning based design methodology for electric machines: Data acquisition, training and optimization," *IEEE Access*, vol. 11, pp. 18 281–18 290, 2023.

[29] V. Parekh, D. Flore, and S. Schöps, "Deep learning-based meta-modeling for multi-objective technology optimization of electrical machines," *IEEE Access*, vol. 11, pp. 93 420–93 430, 2023.

[30] ——, "Deep learning-based prediction of key performance indicators for electrical machines," *IEEE Access*, vol. 9, pp. 21 786–21 797, 2021.

[31] J. C. Gladin, S. Paatel, J. Ahuja, and D. Mavris, "Near zero emissions flight enabled by a robust hybrid-electric architecture," in *AIAA Aviation Forum and Ascend 2024*, 2024, p. 3630.

[32] D. R. Stewart, M. Vatani, R. E. Alden, D. D. Lewis, P. Asef, and D. M. Ionel, "Combined machine learning and differential evolution for optimal design of electric aircraft propulsion motors," in *2024 13th International Conference on Renewable Energy Research and Applications (ICRERA)*. IEEE, 2024, pp. 1823–1828.

[33] W. Hayt and J. Buck, *Engineering Electromagnetics*. McGraw-Hill Companies, Inc., 2012.

[34] P. Asef and A. Lapthorn, "Overview of sensitivity analysis methods capabilities for traction ac machines in electrified vehicles," *IEEE Access*, vol. 9, pp. 23 454–23 471, 2021.

[35] M. Abadi *et al.*, "TensorFlow: Large-scale machine learning on heterogeneous systems," 2015, software available from tensorflow.org. [Online]. Available: https://www.tensorflow.org/